Thresholds for cavitation produced in water by pulsed ultrasound

A.A. Atchley*, L.A. Frizzell, R.E. Apfel, C.K. Holland, S. Madanshetty and R.A. Roy**

Department of Mechanical Engineering, Yale University, PO Box 2159, New Haven, CT 06520, USA

Received 15 November 1987; revised 9 February 1988

The threshold for transient cavitation produced in water by pulsed ultrasound was measured as a function of pulse duration and pulse repetition frequency at both 0.98 and 2.30 MHz. The cavitation events were detected with a passive acoustic technique which relies upon the scattering of the irradiation field by the bubble clouds associated with the events. The results indicate that the threshold is independent of pulse duration and acoustic frequency for pulses longer than approximately 10 acoustic cycles. The threshold increases for shorter pulses. The cavitation events are likely to be associated with bubble clouds rather than single bubbles.

Keywords: cavitation; pulsed ultrasound; water

The potential for the generation of cavitation by pulsed ultrasound has become of increasing concern during the last few years. The major reason for this renewed interest is the widespread use of diagnostic ultrasound in medicine. Apfel[1-3] and Flynn[4,5] have predicted that transient cavitation can occur in liquids irradiated with pulses of ultrasound only a few cycles in duration and there are several reports of cavitation produced by pulsed ultrasound in aqueous media[6,7]. In addition, it has been demonstrated by ter Haar and coworkers that bubbles are caused to grow in mammalian systems which confirms that cavitation nuclei are present [8-10]. Thus, experimental tests of the Apfel and Flynn predictions are considered very important.

A common criterion used as an indicator of cavitation is the generation of free radicals[6,7]. It is the production of free radicals which presents the greatest potential for non-thermal and non-mechanical biological effects. Sono- and chemiluminescence detection[7] and electron spin resonance (ESR) measurements[6] are two methods used to detect the presence of free radicals. Although these methods are useful for detecting cavitation *in vitro*, their use in detecting cavitation in living biological systems is limited. In order for luminescence to be detected, the medium must either be optically transparent or an optical probe must be introduced into the system. ESR measurements cannot be made in real time and are destructive to the sample. In addition, these methods do not detect cavitation directly. The presence of cavitation is inferred from the nature of the onset of free radical production, e.g. the onset has a threshold or the onset is affected by applying static pressure to the system.

In this Paper, we report thresholds for cavitation produced in distilled water by short pulses of ultrasound. The threshold is determined using an acoustical technique which detects cavitation by scattering sound from the bubbles formed during the cavitation event. This detection scheme gives results in real time; the instrumentation is simple; and the medium need only to be acoustically, not optically, transparent. In spite of the fact that the ideal medium for threshold measurements would be a living biological system, measurements in water, such as those to be reported in this Paper, can be used to test the validity of theories that might be applicable to more complex systems.

Experimental apparatus

The apparatus used in this experiment is comprised of two major systems. The sample preparation system is used to prepare the water for the measurements. The electronic instrumentation is used to generate the ultrasonic pulses and detect the cavitation. The sample preparation system is based on a design used previously by two of the authors[11]. The water used in these measurements is tap water which has been distilled, deionized and filtered to 0.2 μm.

The test chamber, pictured in *Figure 1*, is a 40 cm long, 15 cm diameter cylinder comprised of three sections. The two end sections are made of plexiglass, the central section of stainless steel. The left end (in *Figure 1*) of the test chamber is designed to hold the transducer housing, and the right end contains an acoustical absorber to minimize reflections within the chamber. The ends may be partitioned from the central section with thin membranes.

* Permanent address: Physics Department, Naval Postgraduate School, Monterey, CA 93943, USA
** Permanent address: Bioacoustics Research Laboratory, University of Illinois, 1406 W. Green Street, Urbana, IL 61801, USA

Table 2 Results of sonication in early S phase

	Right pouch			Left pouch		
Exposure (W cm^{-2})	Mean number of mitoses per 2000 cells ($\pm$SE)	Number of hamsters	Internally consistent[ab]	Mean number of mitoses per 2000 cells ($\pm$SE)	Number of hamsters	Internally consistent[ab]
0.0	27.6 $\pm$ 3.4	8	No	23.1 $\pm$ 3.3	8	No
0.5	24.5 $\pm$ 2.9	6	Yes	26.7 $\pm$ 2.8	6	Yes
1.0	28.7 $\pm$ 4.0	6	No	27.3 $\pm$ 4.0	6	No
2.5	26.8 $\pm$ 1.6	6	Yes	31.7 $\pm$ 4.6	6	No
5.0	32.0 $\pm$ 2.4	6	Yes	30.7 $\pm$ 2.4	6	No
10.0	26.5 $\pm$ 3.3	6	No	27.2 $\pm$ 3.6	6	No
All	27.7			27.5		

[a] Sonicated
[b] 'No' means the sample points in the data set appear not to have been taken from the same population despite the fact that all animals within a set were similarly treated; for each 'No' the lack of internal consistency is statistically significant at $p < 0.05$

Table 3 Likelihood ratio χ^2 statistics for testing intensity group differences

Phase of cell cycle	Pouch	τ^2	d.f.	Significant[a]	Predicted mean
Late S/ early G_2	Right	6.8	6	No	34.3
	Left	7.3	6	No	33.0
Early S	Right	3.4	5	No	27.7
	Left	4.1	5	No	27.5

[a] $p < 0.05$

for the extra-Poisson variation which we observed. One is that there may be outliers in the data which should be statistically, and hopefully biologically, identified and excluded, leaving homogeneous groups which would allow comparisons of effects at different intensities. The fact that some groups were consistent and some were not supports this alternative. It is also supported to some extent by an examination of the data. The second possibility is that the counts at a given intensity could follow a distribution with greater variability than the Poisson. Indeed there were inconsistent groups with no clear outliers. Furthermore, this would be the situation if the treatment were increasing mitotic variability. We examined both of these possibilities.

We recomputed the χ^2 goodness-of-fit statistics for each intensity group, leaving out each animal in turn. If a non-significant value did not result, pairs of animals were omitted. This procedure produced homogeneous groups. However, there was a lack of consistency between the left and right cheek pouches in the animals identified as outliers, and no biological grounds were apparent for excluding these animals from the analysis.

As a second approach we considered count distributions related to the Poisson but having greater variability. A natural way to incorporate such variability into the statistical model is to allow the mean of the Poisson distribution itself to be random, so that each count is sampled from a distribution which is varying randomly from observation to observation. The most common distribution is the negative binomial[6]. The negative binomial distribution has two parameters: the mean (in this case the mean number of cells in mitosis) and a measure of interanimal homogeneity. We employed a standard statistical program, BMDP3R, to estimate these parameters by the method of maximum likelihood[7]. This approach allowed us to perform likelihood ratio χ^2 tests of differences among the intensity groups for each pouch (left or right) and time of sonication. This was done by comparing the fit of a single negative binomial distribution for all intensity groups to a fit with a different mean for each group but using the same homogeneity parameter. The tests are summarized in *Table 3*. We also calculated Pearson χ^2 goodness-of-fit statistics (by grouping the data) for the overall fit to the early S phase experiments. These were 0.13 (d.f. = 1) for the right pouch and 0.12 (d.f. = 1) for the left, indicating an excellent fit. Mean values predicted by this model are also given in *Table 3* and can be compared with the means in *Tables 1* and *2*. Taken together, the results of these extensive statistical tests clearly indicate the absence of any difference between control and exposed mitotic index.

Acknowledgements

We thank Ms Nancy Stevens for excellent technical assistance during the course of this work. This work was supported in part by USPHS Grant CA39230-14.

References

1 **Miller, MW., Kaufman, G.E., Cataldo, F.L. and Carstensen, E.L.** Absence of mitotic reduction in regenerating rat livers exposed to ultrasound *J Clin Ultrasound* (1976) **4** 169–172
2 **Kremkau, F.W. and Witcofski, R.L.** Mitotic reduction in rat liver exposed to ultrasound *J Clin Ultrasound* (1974) **2** 123–126
3 **Gibbs, S.J. and Casarett, G.W.** Influences of a circadian rhythm and mitotic delay from tritiated thymidine on cytokinetic studies in hamster cheek pouch epithelium *Rad Res* (1969) **40** 588–600
4 **Fry, W.J. and Dunn, F.** Ultrasound: analysis and experimental methods in biological research, in: *Physical Techniques in Biological Research* (Ed Nastuk, W.L.) Academic Press, New York (1962) 261
5 **Bliss, C.** *Statistics in Biology* McGraw-Hill New York (1957) 31
6 **Johnson, N.L. and Kotz, S.** *Distributions in Statistics: Discrete Distributions* Houghton Mifflin Co., Boston (1969) 122
7 **Brown, M.D. and Dixon, W.J.** BMDP Biomedical Computer Programs, P-Series. Health Sciences Computing Facility, UCLA, Los Angeles (1979)

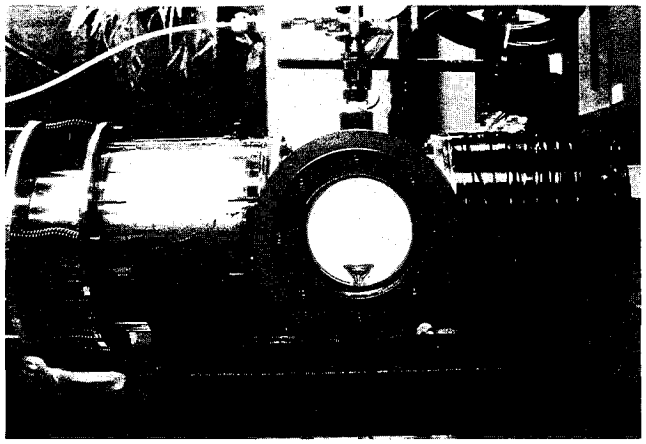

Figure 1 Photograph of the test chamber as seen from the side. The transducer housing is located in the left end of the chamber, the absorber in the right end. The nozzle and sink can be seen through one of the windows. They are located near the top (nozzle) and bottom (sink) of the interior of the test chamber

The central section of the test chamber is a flanged, stainless steel tube, ≈ 10 cm long and 10 cm in diameter. Two glass windows are located in the middle of the tube on either side. These are used as observation ports when aligning the transducer or inspecting the chamber. They can also accommodate a photomultiplier tube or image intensifier to detect sono- or chemiluminescence, or as employed in this experiment, a transducer to acoustically probe the interior of the chamber. The test chamber is also fitted, at the top and bottom, with (Cajon Ultra-torr) O-ring seal vacuum connectors which provide a means of inserting the nozzle (top) and sink (bottom) arrangement, discussed next, into the chamber.

One problem that has consistently plagued cavitation threshold measurements is the specification of the nature, number and location of the cavitation nuclei. The growth of a bubble to a detectable size is a two step process. The first step, the nucleation phase, is the formation of a microbubble from a stabilized nucleus. The second step is the growth of that microbubble. In order to develop an accurate model for the nucleation phase one must have detailed information about the physical properties of the cavitation nuclei present in the medium. Models[1–5] have been developed for the growth phase which is relatively independent of the nucleation mechanism. It is simply assumed in these models that a spherical microbubble of a given radius exists, independent of its origin. Because threshold measurements necessarily involve both steps, it is difficult to make conclusive statements about the validity of the models developed for the growth phase from threshold measurements alone. In order to do so, one must have knowledge concerning the nature of the cavitation nuclei. Such information is usually not known. Therefore, it is commonly assumed that the conditions necessary for nucleation, for at least some of the nuclei, are less stringent than those for the dynamical growth.

Although not resolving this dilemma, we have taken the following approach to introduce some degree of uniformity into the nucleation problem. Cavitation nuclei are most often either gas pockets trapped in cracks or crevices on hydrophobic impurities, or microbubbles which have been stabilized against dissolution. We removed the majority of such 'naturally' occurring cavitation nuclei from the water used in these measurements, by filtration in a closed system consisting of the test chamber and a reservoir described below. During the threshold measurements, hydrophobic, spherical, carboxyl latex particles (1 μm diameter) were introduced at a uniform rate into the focal region of the acoustic field. The intent of using these latex particles is to provide large numbers of the same type of hydrophobic impurity in the region of greatest acoustic intensity during data acquisition. Because it is likely that at least some of these particles contain cavitation nuclei, similar nuclei are present for each phase of the measurement process.

These particles are injected into the test chamber through a coaxial flow arrangement shown in *Figure 2*. The arrangement consists of a hypodermic needle positioned within a tapered glass nozzle (a pipette) having an opening somewhat larger than the bore of the needle. The latex particles are combined with a portion of the filtered, distilled water. A syringe is then filled with the mixture and placed in a syringe pump which delivers a constant volume flow. The nozzle is connected to the filled reservoir. The flow assembly is introduced into the central section of the test chamber through the vacuum connectors mentioned above. By adjusting the syringe pump flow rate and the height of the reservoir connected to the nozzle, a fine coaxial laminar flow can be produced. The inner portion of the flow contains the particles and typically has a diameter on the order of 100 μm. The flow is directed downward through the focal region of the source transducer, as indicated in *Figure 3*, and into a sink which carries the particles out of the test chamber.

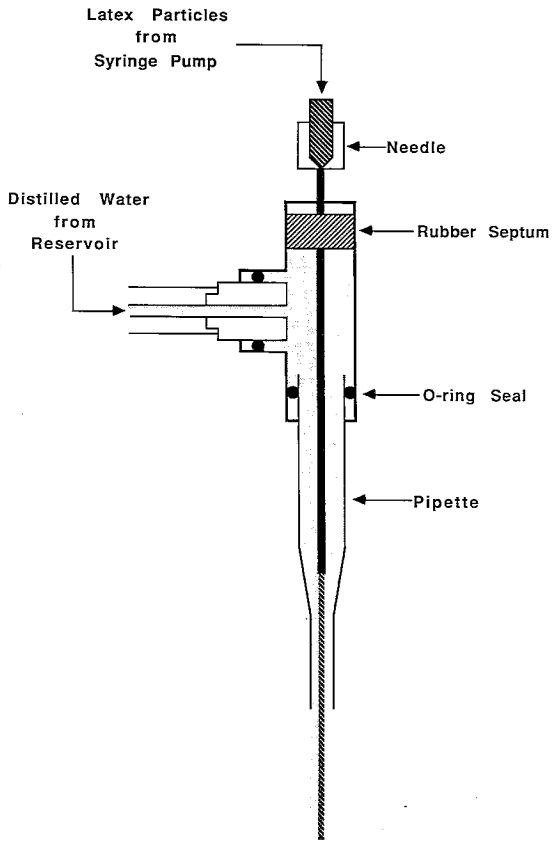

Figure 2 Diagram of the coaxial flow arrangement used to introduce hydrophobic latex spheres into the focal region of the source transducer

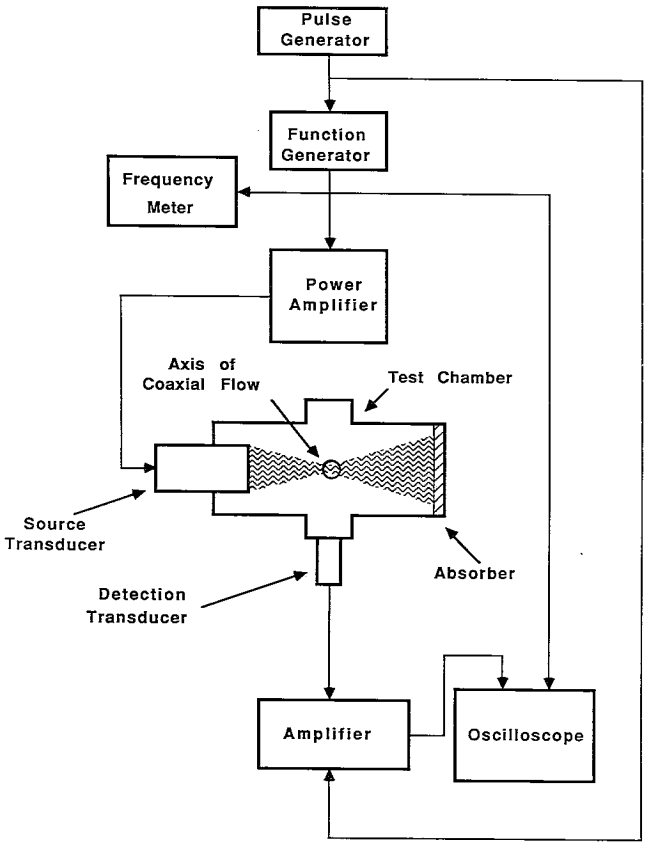

Figure 3 Block diagram of the instrumentation used in this experiment. The section above the test chamber is used to generate the ultrasonic pulses, while that below is used to detect the cavitation

The flow is surprisingly stable and diverges relatively little. The total time required for a parcel of the flow to leave the nozzle, pass through the focus, and enter the sink is typically 1 s or less. Although the flow is disturbed when cavitation occurs in or near it, the disruption is short-lived and seeding of the test chamber with the particles appears to be minimal. In any case, since the flow passes through the focal region, the particles within it have a higher probability of nucleating cavitation events than do stray particles somewhere in a region of lower acoustic intensity. The nozzle and sink can be seen in *Figure 1* near the top (nozzle) and bottom (sink) of the interior of the test chamber.

The electronic instrumentation is divided into two sections, the ultrasound generation system and the cavitation detection system, which are represented schematically in *Figure 3*. The cavitation detection system operates on the principle that the bubbles associated with a cavitation event are strong acoustic scatterers. A pulse from the source transducer produces transient cavitation which results in the formation of a bubble cloud. This bubble cloud will scatter the portions of the pulse that arrive after the cloud's formation and may last long enough to scatter subsequent pulses. The scattered signal is detected by a second transducer which is coupled to one of the viewing windows with acoustic coupling gel.

The processing of the scattered signal takes place as follows. The signal is gated by a rectangular window pulse that is triggered by the excitation pulse sent to the source transducer. The window pulse is delayed by the approximate time required for an acoustic signal to propogate the total distance from the source transducer to the focal region and to the detection transducer. The width of the window is adjusted to be a few pulse durations long. The gated, scattered signal is amplified and sent to an oscilloscope where the operator detects a cavitation event as the appearance of a transient increase in the scattered signal level. This transient is similar in duration to that of the main pulse and usually recurs for several subsequent pulses.

Experimental procedures

Transducer calibration

The calibration of the source transducer involves measuring its total acoustic power output and determining the transverse beam profile at the focus. The total acoustic power is determined from measurement of the deflection of a nearly neutrally buoyant reflecting target, maintained at a 45° angle with respect to the direction of propagation, and which is large enough to intercept all of the energy. The deflection of the target is measured as a function of the peak-to-peak voltage input to the source transducer. The transverse pressure profile is determined using a hydrophone probe and is numerically squared and integrated to find the relation between the total acoustic power output and the peak intensity. The peak intensity is calculated by using this relation and the measured total acoustic power. The peak pressure is calculated from the peak intensity by assuming the plane wave relation. The result of the calibration is the specification of the peak acoustic pressure in terms of the transducer input voltage.

Transducer and coaxial flow alignment

In order for the coaxial flow to be most effective, it must pass through the focus of the source transducer. This alignment is accomplished as follows. A bubble is introduced into the coaxial flow, upstream of the focal region, by squeezing air out of a hypodermic needle introduced into the test chamber through a septum located in one of the windows (not shown in *Figure 1*). If the bubble is small enough it will be trapped in the flow. As the bubble dissolves, the buoyancy force (proportional to the bubble volume) decreases faster than the drag force (proportional to the cross-sectional area) and the bubble slowly moves downstream through the focus. The source is operated in a pulse-echo mode. As the bubble passes near the focal region, the transducer axis is adjusted relative to the coaxial flow axis until the signal scattered from the bubble is maximized. Since an individual bubble remains in the focal region for only a short time, a number of bubbles must be used in order to complete the alignment procedure. After an individual bubble has passed through the focal region it is removed from the flow and another bubble is introduced. The speed of the flow and the gas content of the liquid in the chamber both remain constant during the alignment procedure so that all of the bubbles are the same size when they pass through the focus. Therefore, the scattering strength of each bubble is the same.

Sample preparation

The sample preparation procedure consists of filling the system with distilled, deionized water, degassing the water and preparing the latex particles. Once the system is filled, the water is circulated through a 0.2 μm filter for $\approx$ 15 min in order to remove any solid contaminants that might

have been in the system prior to filling. The flow rate through the filter is ≈ 1 dm^3 min^{-1}; the system capacity is ≈ 5 dm^3. Hence, a typical parcel of water passes through the filter about three times. After the filtration is completed, the water is degassed. This process involves circulating the water while the degassing reservoir is held at a reduced pressure, typically ≈ 0.2 bar* (absolute). During the degassing process the filter is bypassed and the flow rate is increased so that there is sufficient agitation in the reservoir. The process continues until all visible bubbles in the test chamber have dissolved, a condition which usually occurs after ≈ 45 min. When the bubbles disappear, the reservoir is returned to atmospheric pressure and the circulation stopped. The cavitation threshold of water prepared in this manner is typically ≈ 30 bar, or a factor of at least two higher than the thresholds measured using the coaxial jet containing the latex particles.

The latex particles are supplied 4% by weight in distilled water. They are diluted further by adding ≈ 1 ml of the 4% mixture to 20 ml of water drawn from the degassed system. This stock mixture is refrigerated. When needed for a measurement, the stock mixture is removed from the refrigerator and degassed for ≈ 2 min, after which 3 ml of the mixture is drawn into a sterile disposable syringe. The syringe is placed in a syringe pump and connected to the inlet of the coaxial flow. During data acquisition the nuclei are pumped out of the syringe at a rate of ≈ 1 ml h^{-1}.

Data acquisition

The cavitation threshold is defined to be the peak pressure amplitude at which a transient in the scattered signal is first observed. During data acquisition, the amplitude of the pulse is manually ramped until a cavitation event is detected. Once an event is detected, the input voltage to the power amplifier is recorded and the amplitude reduced to zero. Following a 1 min wait period, the ramping procedure is repeated until at least 10 threshold measurements have been made for a given set of pulse parameters (pulse duration and pulse repetition frequency).

Results

The cavitation threshold was measured for several values of the pulse duration and pulse repetition frequency (PRF) for 0.98 and 2.30 MHz ultrasound. The results of the measurements are presented in *Figure 4–7*. The data points represent the average of at least 10 and as many as 60 individual threshold measurements. The error bars correspond to plus or minus one standard deviation.

The dependence of the threshold on pulse duration for 0.98 MHz ultrasound is shown in *Figure 4* for both 200 and 1000 Hz PRF. The threshold for each PRF is independent of pulse duration for pulses longer than ≈ 10 μs, that is, for pulses longer than approximately 10 acoustic cycles. The cavitation threshold increases approximately linearly with decreasing logarithm of the pulse duration for shorter pulses. Although the threshold is about 3 bar lower at 200 Hz PRF than at 1000 Hz for longer pulse durations, the difference in the threshold diminishes at shorter pulse durations.

Figure 5 is a graph of the threshold *versus* pulse duration at 0.98 MHz for the 10 and 20% duty cycle.

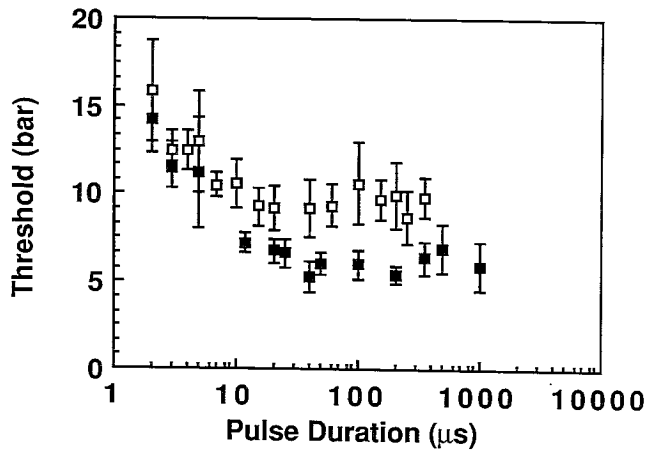

Figure 4 Variation of the cavitation threshold with pulse duration (plotted on a logarithmic scale) at constant pulse repetition frequency (PRF). The acoustic frequency is 0.98 MHz. ■, 200 Hz PRF; □, 1000 Hz PRF

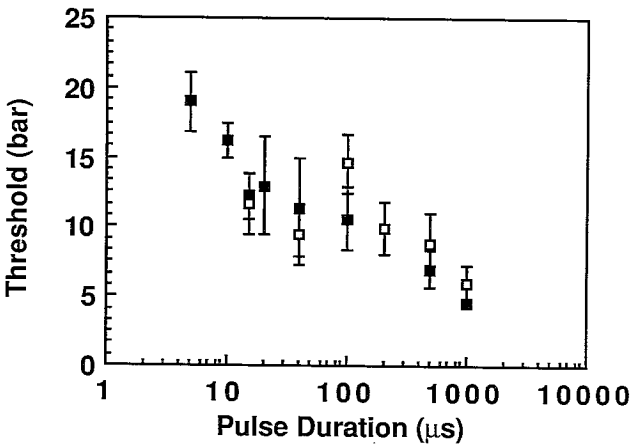

Figure 5 Variation of the cavitation threshold with pulse duration (plotted on a logarithmic scale) at constant duty cycle. The acoustic frequency is 0.98 MHz. ■, 10% duty cycle; □, 20% duty cycle

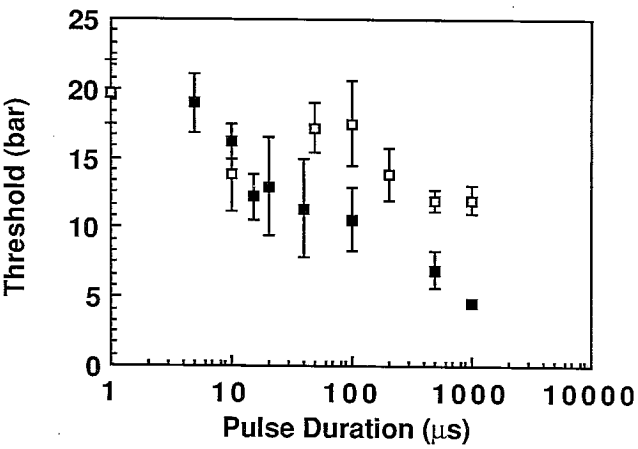

Figure 6 Variation of the cavitation threshold with pulse duration (plotted on a logarithmic scale) at 10% duty cycle. ■, 10% duty cycle from *Figure 5*; □, thresholds for chemiluminescence emission under similar acoustic conditions measured by Crum and Fowlkes[7]

The threshold is essentially the same for the two duty cycles. The 10% duty cycle data have been reproduced in *Figure 6* along with similar data published by Crum and Fowlkes[7] who used chemiluminescence detection to determine the threshold. Our measurements indicate a lower threshold at longer pulse durations, perhaps related

*1 bar = 10^2 kPa

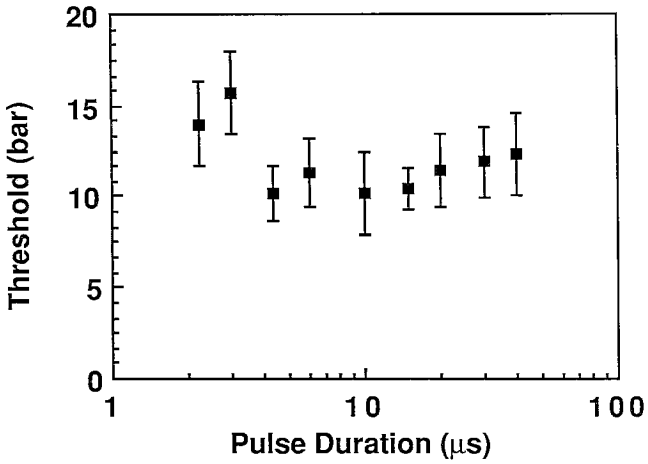

Figure 7 Variation of the cavitation threshold with pulse duration (plotted on a logarithmic scale) at 2.30 MHz and 1000 Hz PRF

to our use of latex particles. In addition, our values display a greater sensitivity to changes in pulse duration.

The variation in the threshold with pulse duration at 2.30 MHz and 1000 Hz PRF is shown in *Figure 7*. The threshold is essentially independent of pulse duration for pulses longer than ≈ 4 μs and increases with decreasing logarithm of the pulse duration for shorter pulses. A 4 μs pulse is approximately 9 acoustic cycles in duration at 2.30 MHz. This behaviour is similar to that for the corresponding 0.98 MHz data shown in *Figure 4*.

Discussion

The fact that there is little difference in the cavitation threshold for 0.98 and 2.30 MHz ultrasound is consistent with the theories of Apfel and Flynn. According to these theories, frequency dependent effects start to become important at around 5 MHz, but only for viscosities approximately 10 times that of water. No frequency dependence is apparent in our threshold measurements. In order to further confirm the theories, higher frequencies and more viscous fluids should be used.

The pulse amplitudes at which we observe cavitation are within the range of amplitudes used in diagnostic instruments. In terms of peak intensities, the thresholds reported in this Paper range from ≈ 10 to 120 W m^{-2}. However, these results for water cannot be applied to the mammalian system. They only indicate the need for further investigation of cavitation thresholds in mammals.

The data presented in *Figures 4* and *7* indicate that for pulses longer in duration than about 10 acoustic cycles, the threshold is relatively independent of pulse duration and acoustic frequency. As mentioned above, the lack of dependence on acoustic frequency is predicted by theory. The transition at 10 cycles suggests that there is some type of evolution, such as rectified diffusion, which is completed after approximately 10 cycles.

Our acoustically based thresholds are in fair agreement with the chemiluminescence based thresholds of Crum and Fowlkes, although the data diverge at longer pulse durations. Because our system is likely not sensitive enough to detect the sound scattered from a single bubble, a typical event is probably associated with the formation of a bubble cloud. Because the thresholds are similar, it is possible that the same type of events were detected in both experiments, i.e. measurable levels of chemiluminescence are also associated with a bubble cloud, rather than an individual bubble. This conclusion is supported by the fact that our thresholds are usually lower than those measured by Crum and Fowlkes. (However, it must be pointed out that the differences in the threshold may be attributable to differences in the sample water. Crum and Fowlkes used a luminol/sodium hydroxide/distilled water solution containing 'natural' cavitation nuclei while we used distilled water containing latex particles.) Because theoretical thresholds are based on single bubble models, the conclusion that the observed cavitation events are associated with bubble clouds may have important implications and warrants further investigation.

It must be pointed out that the exact influence of the hydrophobic latex particles, and of the coaxial flow arrangement itself, is not well understood. The intent of using the latex particles is to provide large numbers of the same type of hydrophobic impurity in the focal region of the source transducer during data acquisition in order to introduce a degree of uniformity into the cavitation process. Even so the exact nucleation mechanism is unknown. If indeed the cavitation events detected are due to nuclei associated with the latex particles, it is clear that every particle does not contain the same type of cavitation nucleus. If they did, then once the cavitation threshold was exceeded each particle would trigger an event. This is not the case. In fact, many particles pass through the focal region before a cavitation event is detected. Therefore, the nuclei are probably related to some irregularity associated with the spherical particles, such as an imperfectly wetted deformation or a gas pocket trapped by an agglomeration of particles. In any case, the cavitation threshold of the water in the absence of the coaxial flow containing the particles is approximately a factor of two higher than that with the flow. In addition, with the flow the threshold measurements are reproducible to within $\approx 15\%$, which is good for measurements of this type.

One important feature of the detection technique employed in this project is that it is capable of providing information, although qualitative, about the time evolution of the cavitation events. This information could be gained by analysing the time evolution of the scattered signal. Also, the use of this system in conjunction with a luminescence detection system could yield information concerning the correlation between luminescence intensity and the size of the scattering bubble cloud.

Acknowledgements

This work was supported in part by grants from the National Institutes of Health. In addition, A. A. Atchley was supported by the Acoustical Society of America's F. V. Hunt Postdoctoral Fellowship for which he is deeply indebted.

A. A. Atchley and L. A. Frizzell, who were visiting Yale University on a postdoctoral fellowship and on sabbatical leave, respectively, wish to thank the co-authors for their hospitality, the use of their facilities and their generous provision of time and effort which made this study possible.

References

1 **Apfel, R.E.** Acoustic cavitation prediction *J Acoust Soc Am* (1981) **69** 1624–1633

2 **Apfel, R.E.** Acoustic cavitation: a possible consequence of

biomedical uses of ultrasound *Br J Cancer* (1982) **45** (Suppl V) 140–146

3 **Apfel, R.E.** Possibility of microcavitation from diagnostic ultrasound *IEEE Trans Ultrasonics, Ferroelectrics, Freq Control* (1986) **UFFC-33** 139–142

4 **Flynn, H.G.** Generation of transient cavities in liquids by microsecond pulses of ultrasound *J Acoust Soc Am* (1982) **72** 1926–1932

5 **Carstensen, E.L. and Flynn, H.G.** The potential for transient cavitation with microsecond pulses of ultrasound *Ultrasound Med Biol* (1982) **8** L720–L724

6 **Carmichael, A.J., Massoba, M.M., Reisz, P. and Christman, C.L.** Free radical production in aqueous solutions exposed to simulated ultrasonic diagnostic conditions *IEEE Trans Ultrasonics, Ferroelectrics, Freq Control* (1986) **UFFC-33** 148–155

7 **Crum, L.A. and Fowlkes, J.B.** Acoustic cavitation generated by microsecond pulses of ultrasound *Nature* (1986) **319** 52–54

8 **ter Haar, G.R. and Daniels, S.** Evidence for ultrasonically induced cavitation *in vivo Phys Med Biol* (1981) **26** 1145–1149

9 **ter Haar, G.R., Daniels, S., Eastaugh, K.C. and Hill, C.R.** Ultrasonically induced cavitation *in vivo Br J Cancer* (1982) **45** (Suppl V) 151–155

10 **ter Haar, G.R., Daniels, S. and Morton, K.** Evidence for acoustic cavitation *in vivo*: thresholds for bubble formation with 0.75 MHz continuous wave and pulsed beams *IEEE Trans Ultrasonics, Ferroelectrics, Freq Control* (1986) **UFFC-33** 162–164

11 **Roy, R.A., Atchley, A.A., Crum, L.A., Fowlkes, J.B. and Reidy, J.J.** A precise technique for the measurement of acoustic cavitation thresholds and some preliminary results *J Acoust Soc Am* (1985) **78** 1799–1805